www.sciencemag.org/content/347/6228/1374/suppl/DC1

Supplementary Materials for

A mitochondrial UPR-mediated metabolic checkpoint regulates hematopoietic stem cell aging

Mary Mohrin, Jiyung Shin, Yufei Liu, Katharine Brown, Hanzhi Luo, Yannan Xi, Cole M. Haynes, Danica Chen*

*Corresponding author. E-mail: danicac@berkeley.edu

Published 20 March 2015, *Science* **347**, 1374 (2015)
DOI: 10.1126/science.aaa2361

This PDF file includes:

Materials and Methods

Cell culture and RNAi

293T cells were acquired from the ATCC. Cells were cultured in advanced DMEM (Invitrogen) supplemented with 1% penicillin-streptomycin (Invitrogen) and 10% FBS (Invitrogen). For inducing PFS^{mt}, cells were treated with doxycycline (30 ug/mL) for 48 hrs, or ethidium bromide (50 ng/mL) for 7 days. Alternatively, cells were transfected with a construct expressing an aggregation prone mutant mitochondrial OTC protein from the Hoogenraad lab (*18*). For nutrient deprivation, cells were cultured in glucose free medium (Invitrogen) or glutamine free medium (Invitrogen) for 48-68 hours. Cell proliferation and survival were scored using a Vi-Cell Analyzer (Beckman Coulter).

SIRT7 knockdown target sequences are as follows, as previously described (*9*):

S7KD1, 5'-CACCTTTCTGTGAGAACGGAA-3';

S7KD2, 5'-TAGCCATTTGTCCTTGAGGAA-3',

NRF1 knockdown target sequences are as follows:

NRF1 KD (mouse), 5'-GAAAGCTGCAAGCCTATCT-3'

NRF1 KD (human), 5'-CACCGTTGCCCAAGTGAATTA-3'

Double-stranded siRNAs were purchased from Thermo Scientific and were transfected into cells via RNAiMax (Invitrogen) according to manufacturer's instructions. Generation of SIRT7 knockdown and overexpressing cells was described previously (*9*). After puromycin selection, cells were recovered in puromycin free medium for 2-3 passages before analyses.

Measurements of mitochondrial mass, ATP, citrate synthase activity, and oxygen consumption

To measure mitochondrial mass, cells were stained with 100nM MitoTracker Green (Invitrogen) for 30 minutes in at 37°C, and analyzed with flow cytometry (BD Fortessa).

For oxygen consumption, $3X10^5$ cells were plated using CellTak (BD) and the oxygen consumption rate (OCR) was measured using a Seahorse XF24 instrument following the manufacturer's instructions (Seahorse Biosciences). OCR was measured under basal conditions, in the presence of the mitochondrial inhibitor oligomycin A (1 uM), mitochondrial uncoupler FCCP (1 uM) and respiratory chain inhibitor antimycin and rotenone (1 uM).

Citrate synthase activity was measured following the manufacturer's instruction (Biovision Citrate Synthase Activity Colorimetric Assay Kit #K318-100). To measure ATP, cells in suspension were mixed with an equal volume of CellTiterGlo in solid white luminescence plates (Grenier Bio-One) following the manufacturer's instructions (Promega). Luminescence was measured using a luminometer (LMAX II 384 microplate reader, Molecular Devices) to obtain relative luciferase units (RLU).

Co-immunoprecipitations

Co-immunoprecipitations were performed as previously described (*14*) with Flag-resin (Sigma) or Protein A/G beads (Santa Cruz) for SIRT7 IP. Elution was performed with

either Flag peptide (Sigma) or 100mM Glycine solution (pH 3) for SIRT7 IP. Antibodies are provided in Table S1.

ChIP and mRNA analysis

Cells were prepared for ChIP as previously described (*26*), with the exception that DNA was washed and eluted using a PCR purification kit (Qiagen) rather than by phenol-chloroform extraction. RNA was isolated from cells or tissues using Trizol reagent (Invitrogen) and purified using the RNeasy Mini Kit (Qiagen). cDNA was generated using the qScript™ cDNA SuperMix (Quanta Biosciences). Gene expression was determined by real time PCR using Eva qPCR SuperMix kit (BioChain Institute) on an ABI StepOnePlus system. All data were normalized to ActB or GAPDH expression. Antibodies and PCR primer details are provided in Table S1-3.

Mice

SIRT7$^{-/-}$ mice have been described previously (*9*). All mice were housed on a 12:12 hr light:dark cycle at 25°C. For 5-Fluorouricil treatment study, 1x10^{6} BMCs from SIRT7$^{+/+}$ or SIRT7$^{-/-}$ mice were transplanted into lethally irradiated recipient mice. 4 months posttransplantation, 5-Fluorouricil was administrated to mice intraperitoneally at a dose of 150 mg/kg once per week, and the survival of the mice was monitored daily. All animal procedures were in accordance with the animal care committee at the University of California, Berkeley.

Flow Cytometry and Cell Sorting

BMCs were obtained by crushing the long bones with sterile PBS without calcium and magnesium supplemented with 2% FBS. Lineage staining contained a cocktail of biotinylated anti-mouse antibodies to Mac-1 (CD11b), Gr-1 (Ly-6G/C), Ter119 (Ly-76), CD3, CD4, CD8a (Ly-2), and B220 (CD45R) (BioLegend). For detection or sorting, we used streptavidin conjugated to APC-Cy7, c-Kit-APC, Sca-1-Pacific blue, CD48-FITC, and CD150-PE (BioLegend). For congenic strain discrimination, anti-CD45.1 PerCP and anti-CD45.2 PE-Cy7 antibodies (BioLegend) were used. For assessment of apoptosis and cell cycle analysis, AnnexinV and Ki-67 (BioLegend) staining were performed respectively according to the manufacturer's recommendation after cell surface staining. For in vivo cell-cycle analysis, BrdU (Invitrogen) was incorporated over a 16-hour period. For ex vivo proliferation analysis, cultured BMCs were pulsed with BrdU (Invitrogen) for one hour before flow cytometry analysis. For mitochondrial mass, BMCs were incubated with 100nM MitoTracker Green (Invitrogen) for 30 min at 37°C in the dark after cell surface staining. All data were collected on a Fortessa (Becton Dickinson), and data analysis was performed with FlowJo (TreeStar). For cell sorting, lineage depletion or c-kit enrichment was performed according to the manufacturer's instructions (Miltenyi Biotec). Cells were sorted using a Cytopeia INFLUX Sorter (Becton Dickinson). Antibody details are provided in Table S1.

Lentiviral Transduction of HSCs

As previously described (*27*), sorted HSCs were prestimulated for 5-10 hrs in a 96 well U bottom dish in StemSpan SFEM (Stem Cell Technologies) supplemented with 10% FBS (Stem Cell Technologies), 1% Penicillin/Streptomycin (Invitrogen), IL3 (20ng/ml), IL6

(20ng/ml), TPO (50ng/ml), Flt3L (50ng/ml), and SCF (100ng/ml) (Peprotech).

SIRT7 was cloned into the pFUGw lentiviral construct. NRF1 shRNA was cloned into pFUGw-H1 lentiviral construct. Lentivirus was produced as described (*14*), concentrated by centrifugation, and resuspended with supplemented StemSpan SFEM media. The lentiviral media were added to HSCs in a 24 well plate, spinoculated for 90 min at 270g in the presence of 8ug/ml polybrene. This process was repeated 24 hr later with a fresh batch of lentiviral media.

mtDNA/nDNA

The mitochondrial DNA/nuclear DNA (mtDNA/nDNA) ratio was determined by isolating DNA from cells with Trizol (Invitrogen), as described previously (*28*). The ratio of mtDNA/nDNA was calculated as previously described (*29*).

Electron Microscopy

40,000 HSCs were pelleted at 150g. Samples were fixed with 2% gluaraldehyde for 10 minutes at room temperature while rocking. Samples were pelleted at 600g and further fixed with 2% glutaraldehyde / 0.1M NaCacodylate at 4°C and were submitted to the UC Berkeley Electron Microscope Core Facility for standard transmission electron microscopy ultrastructure analyses.

Transplantation Assays

For transplantations, $5x10^5$ BMCs from $SIRT7^{+/+}$ or $SIRT7^{-/-}$ CD45.2 littermates was

mixed with $5x10^5$ CD45.1 B6.SJL (Jackson Laboratory) competitor BMCs and injected into lethally irradiated (950 Gy) CD45.1 B6.SJL recipient mice. Alternatively, 250 sorted HSCs from $SIRT7^{+/+}$ or $SIRT7^{-/-}$ mice were mixed with $5x10^5$ CD45.1 B6.SJL competitor BMCs and injected into lethally irradiated B6.SJL recipient mice. To assess multilineage reconstitution of transplanted mice, peripheral blood was collected every month for 4 months by retroorbital bleeding. Red blood cells were lysed and the remaining blood cells were stained with CD45.2 FITC, CD45.1 PE, Mac1 PerCP, Gr1 Cy7PE, B220 APC, and CD3 PB (Biolegend). Antibody details are provided in Table S1.

Statistical Analysis

The number of mice chosen for each experiment is based on the principle that the minimal number of mice is used to have sufficient statistical power and is comparable to published literature for the same assays performed. Mice were randomized to groups and analysis of mice and tissue samples were performed by investigators blinded to the treatment of genetic background of the animals. Transplant experiments have been repeated 5 times. HSC characterizations in $SIRT7^{-/-}$ mice have been repeated in 10 different cohorts of mice. Analyses in SIRT7 KD cells have been repeated 2-5 times. Experiments are repeated by at least 2 different scientists. Statistical analysis was performed with Excel (Microsoft) and Prism 5.0 Software (GraphPad Software). Means between two groups were compared with two-tailed, unpaired Student's t-test. Error Bars represent standard errors. In all corresponding figures, * represents $p<0.05$. ** represents $p<0.01$. *** represents $p<0.001$. ns represents $p>0.05$.

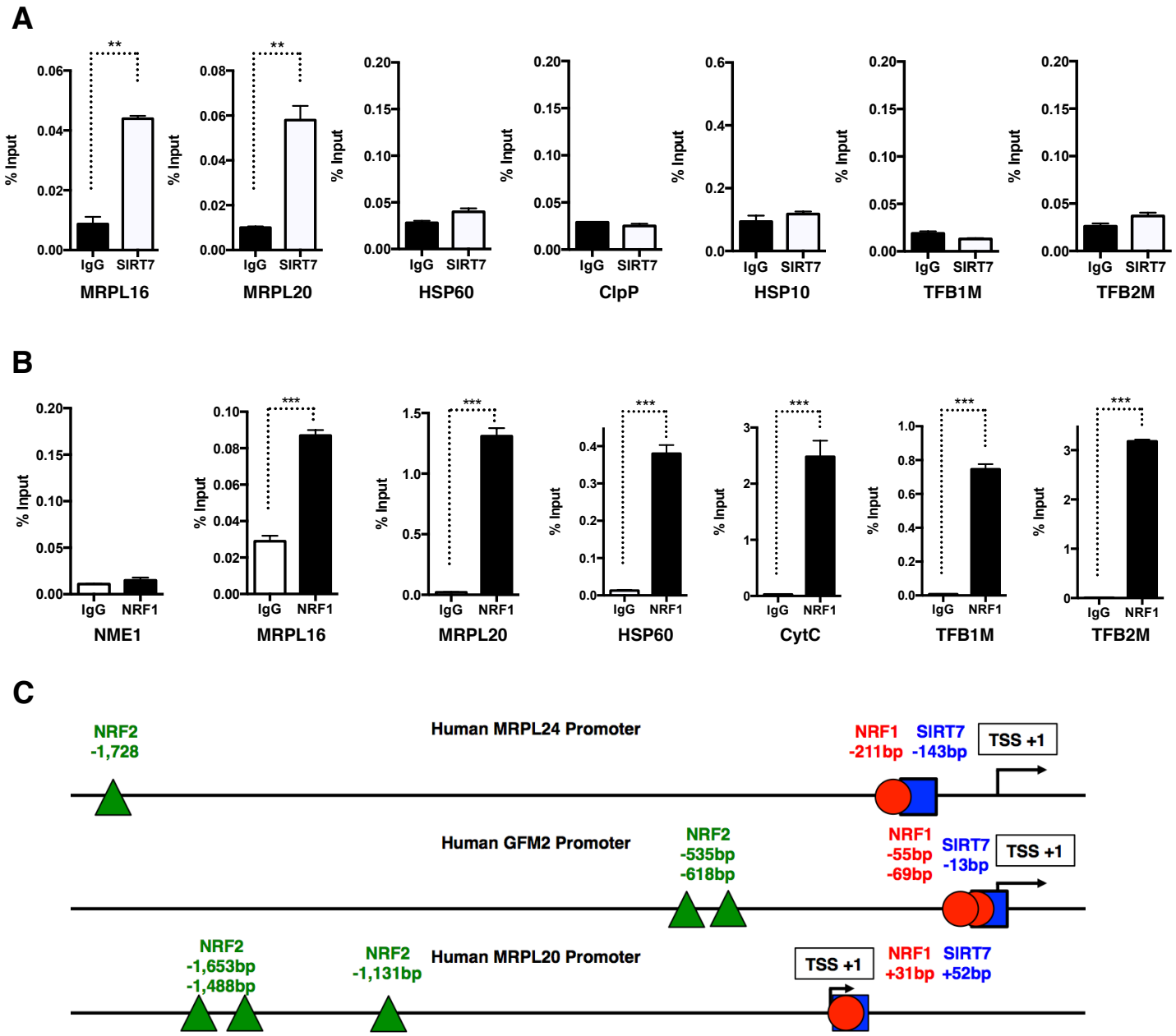

Fig. S1. SIRT7 and NRF1 co-occupy the same genomic regions at the promoters of mitochondrial translation machinery components.

(**A** and **B**) SIRT7 binds the promoters of mRPs but not other mitochondrial genes. NRF1 binds the promoters of mRPs and other mitochondrial genes, but not NME1, a known target of SIRT7. SIRT7 and NRF1 occupancy at gene promoters in 293T cells was determined by ChIP-PCR, compared to IgG negative control samples. All samples were normalized to input DNA.

(**C**) Schematic representation of NRF1 and NRF2 consensus binding sequences, and SIRT7 binding sites at gene promoters. SIRT7 binding sites were determined in a ChIP-seq study (Barber et al. Nature 2012).

Error bars represent SE. **: $p<0.01$. ***: $p<0.001$.

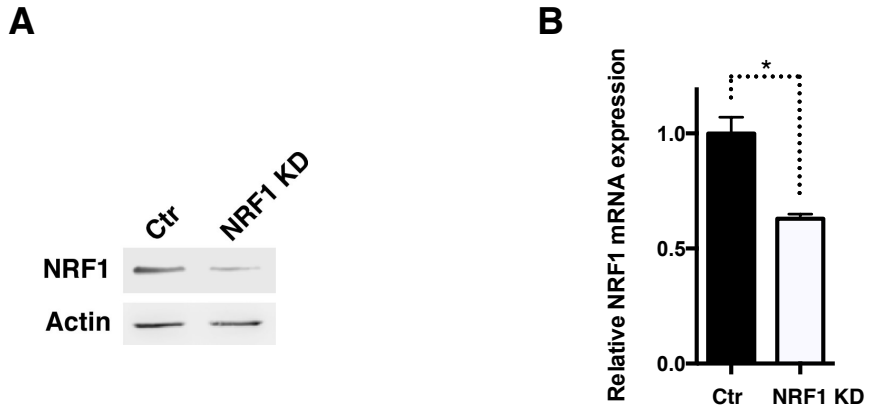

Fig. S2. Knockdown of NRF1 with siRNA in cells.

(**A** and **B**) NRF1 siRNA reduces the expression by 40%. 293T cells were transfected with NRF1 siRNA. The expression levels of NRF1 were determined by immunoblots and qPCR. Error bars represent SE. *: $p<0.05$.

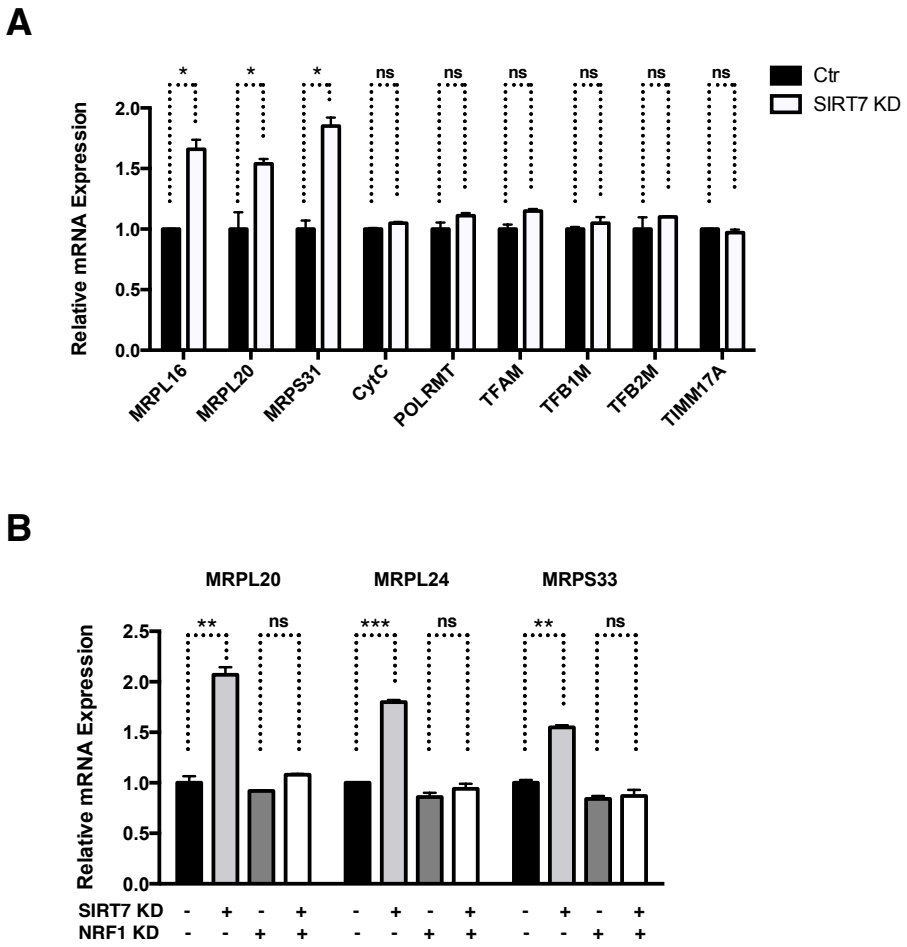

Fig. S3. SIRT7 represses NRF1 transcription.

(**A**) SIRT7 represses the expression of mRPs. SIRT7 was knocked down in 293T cells via shRNA. Gene expression in SIRT7 KD cells and control cells was determined by qPCR.
(**B**) SIRT7 represses the expression of mRPs via NRF1. SIRT7 KD 293T cells and control cells were treated with control or NRF1 siRNA as indicated. Gene expression was determined by qPCR. NRF1 KD abrogates SIRT7-mediated transcriptional repression of mRPs in cells.
Error bars represent SE **: $p<0.01$. ***: $p<0.001$. ns: $p>0.05$

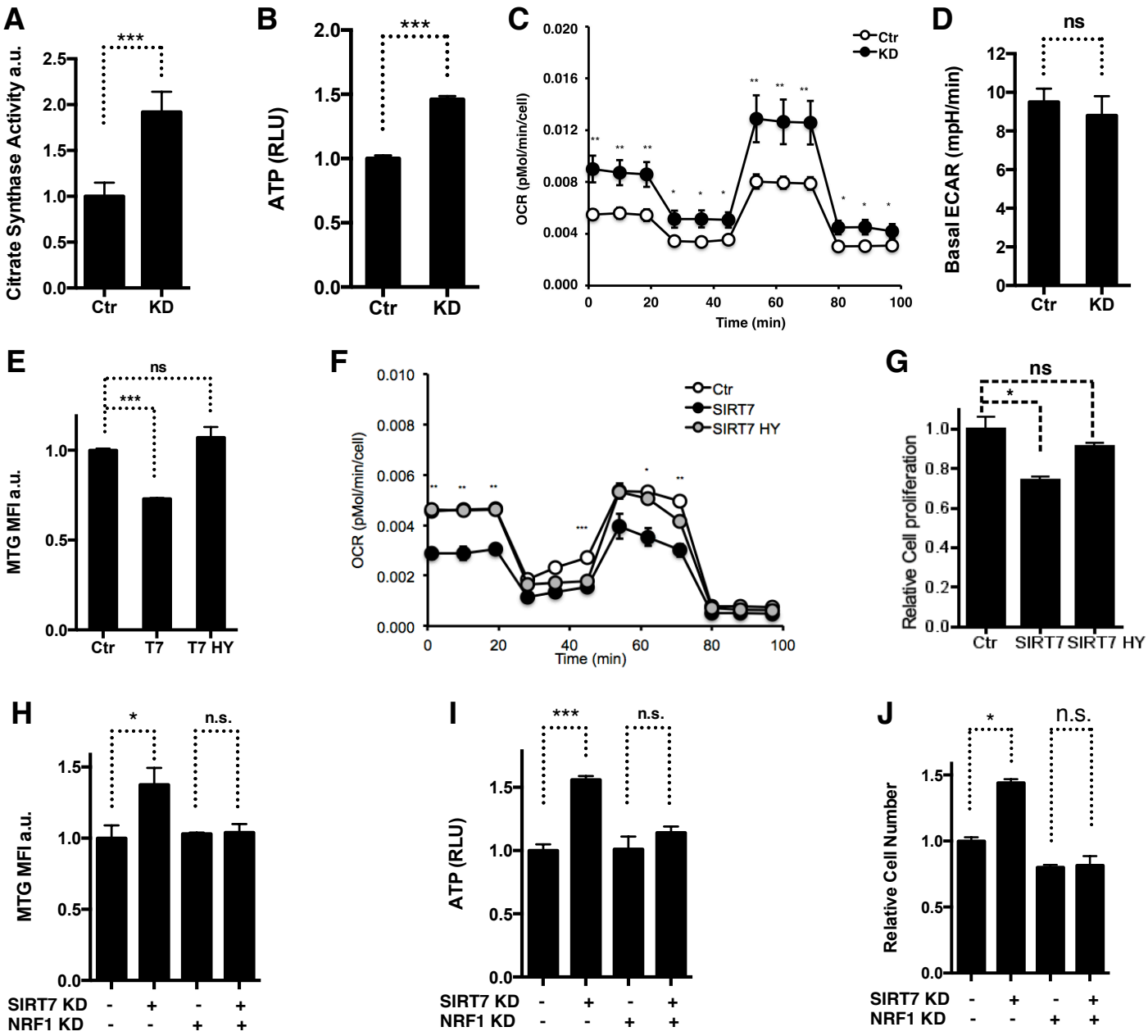

Fig. S4. SIRT7 limits mitochondrial activity and cell proliferation.

(**A** to **D**) Increased mitochondrial activity in SIRT7 KD cells. Comparison of SIRT7 KD 293T cells and control cells for citrate synthase activity quantification (A), cellular ATP quantification using a luminescent assay (B), and Seahorse analyses (C and D). OCR, oxygen consumption rate. ECAR, extracellular acidification rate.

(**E** to **G**) Overexpression of WT but not a catalytically inactive mutant (HY) SIRT7 reduces mitochondrial activity and proliferation. Comparison of 293T cells overexpressing WT and mutant SIRT7 and control cells for MTG staining (E), Seahorse analyses (F), and cell proliferation analyses (G). Cells were counted using a Vi-Cell analyzer.

(**H** to **J**) NRF1 siRNA restores increased mitochondrial activity and proliferation in SIRT7 KD cells. SIRT7 KD 293T cells and control cells treated with control or NRF1 siRNA were analyzed for MTG staining (H), cellular ATP quantification (I), and cell proliferation analyses (J).

Error bars represent SE *: $p<0.05$. **: $p<0.01$. ***: $p<0.001$. ns: $p>0.05$.

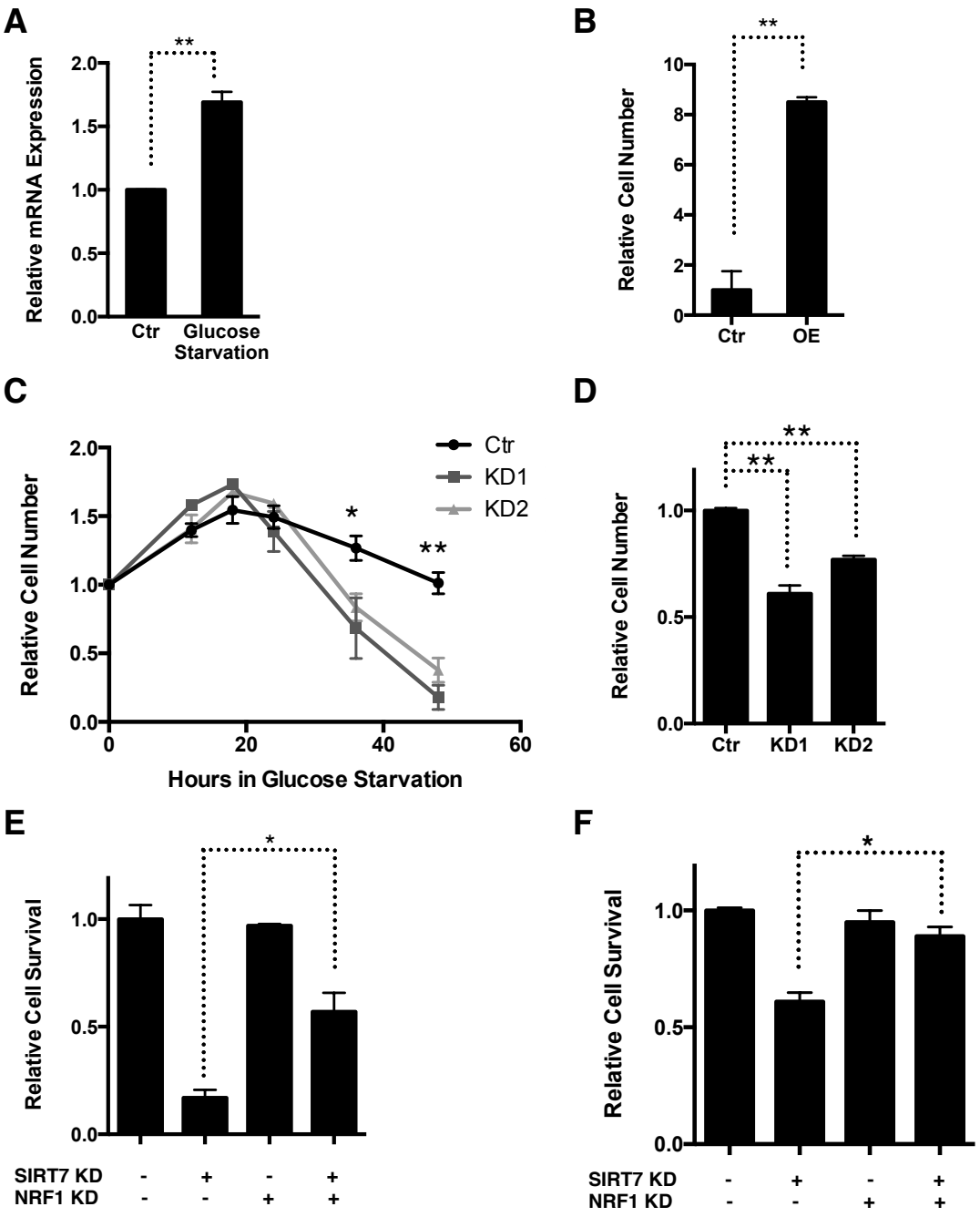

Fig. S5. SIRT7 promotes nutritional stress resistance.

(**A**) SIRT7 expression is increased upon glucose starvation. qPCR comparing SIRT7 expression in 293T cells growing in medium containing 25mM glucose and without glucose.
(**B** to **D**) SIRT7 increases nutrient starvation stress resistance. SIRT7 OE 293T cells and control cells were deprived of glucose for 68 hours (B). SIRT7 KD 293T cells and control cells were deprived of glucose (C) and glutamine (D) for 48 hours. Cells were counted using a Vi-Cell analyzer.
(**E** and **F**) NRF1 KD attenuates the sensitivity of SIRT7 deficient cells to glucose (E) or glutamine (F) starvation. SIRT7 KD 293T cells and control cells were treated with control or NRF1 siRNA. Cells were deprived of glucose or glutamine for 48 hours. Cells were counted using a Vi-Cell analyzer.
Error bars represent SE *: $p<0.05$. **: $p<0.01$.

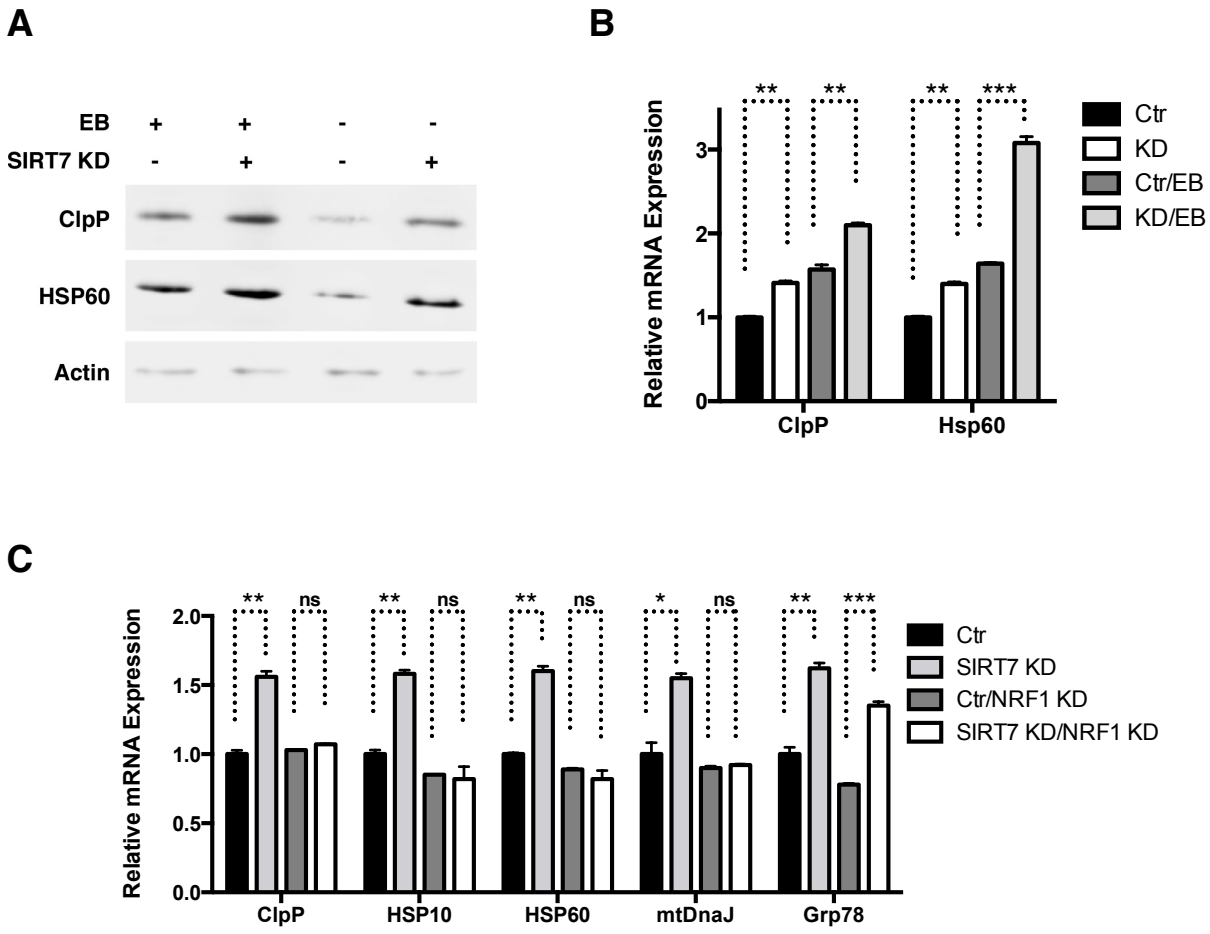

Fig. S6. SIRT7 represses NRF1 activity to suppress PFS^{mt}.

(**A** and **B**) SIRT7 represses PFS^{mt}. SIRT7 KD 293T cells and control cells were treated with or without EB for 7 days. The expression of UPR^{mt} genes (ClpP and HSP60) were determined by immunoblots (A) or qPCR (B).

(**C**) SIRT7 represses NRF1 activity to suppress PFS^{mt}. SIRT7 KD 293T cells and control cells were treated with control or NRF1 siRNA. The expression of UPR^{mt} (ClpP, HSP10, HSP60, mtDnaJ) and UPR^{ER} genes (Grp78) was determined by qPCR.

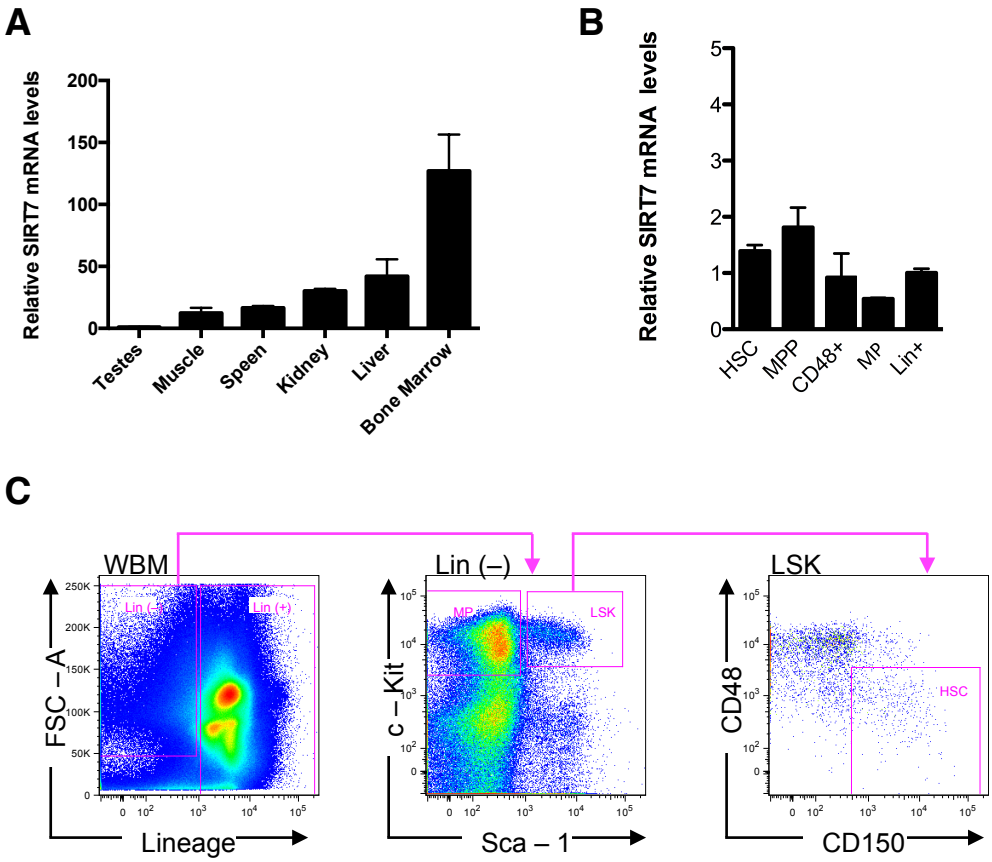

Fig. S7. SIRT7 expression in various tissues and cellular compartments.

(**A**) SIRT7 is highly expressed in the bone marrow. The expression of SIRT7 in various tissues was compared by qPCR.
(**B**) SIRT7 is ubiquitously expressed in various hematopoietic cellular compartments in the bone marrow. Various cell populations in the bone marrow were isolated via cell sorting based on cell surface markers. HSC, Lin$^-$c-Kit$^+$Sca1$^+$CD150$^+$CD48$^-$; multipotent progenitors (MPPs), Lin$^-$c-Kit$^+$Sca1$^+$CD150$^-$ CD48$^-$; CD48+, Lin$^-$c-Kit$^+$Sca1$^+$CD48$^+$; myeloid progenitors (MPs), Lin$^-$c-Kit$^+$Sca1$^-$; and differentiated blood cells, Lin$^+$. The expression of SIRT7 was determined by qPCR.
(**C**) Gating strategy for sorting HSCs.
Error bars represent SE.

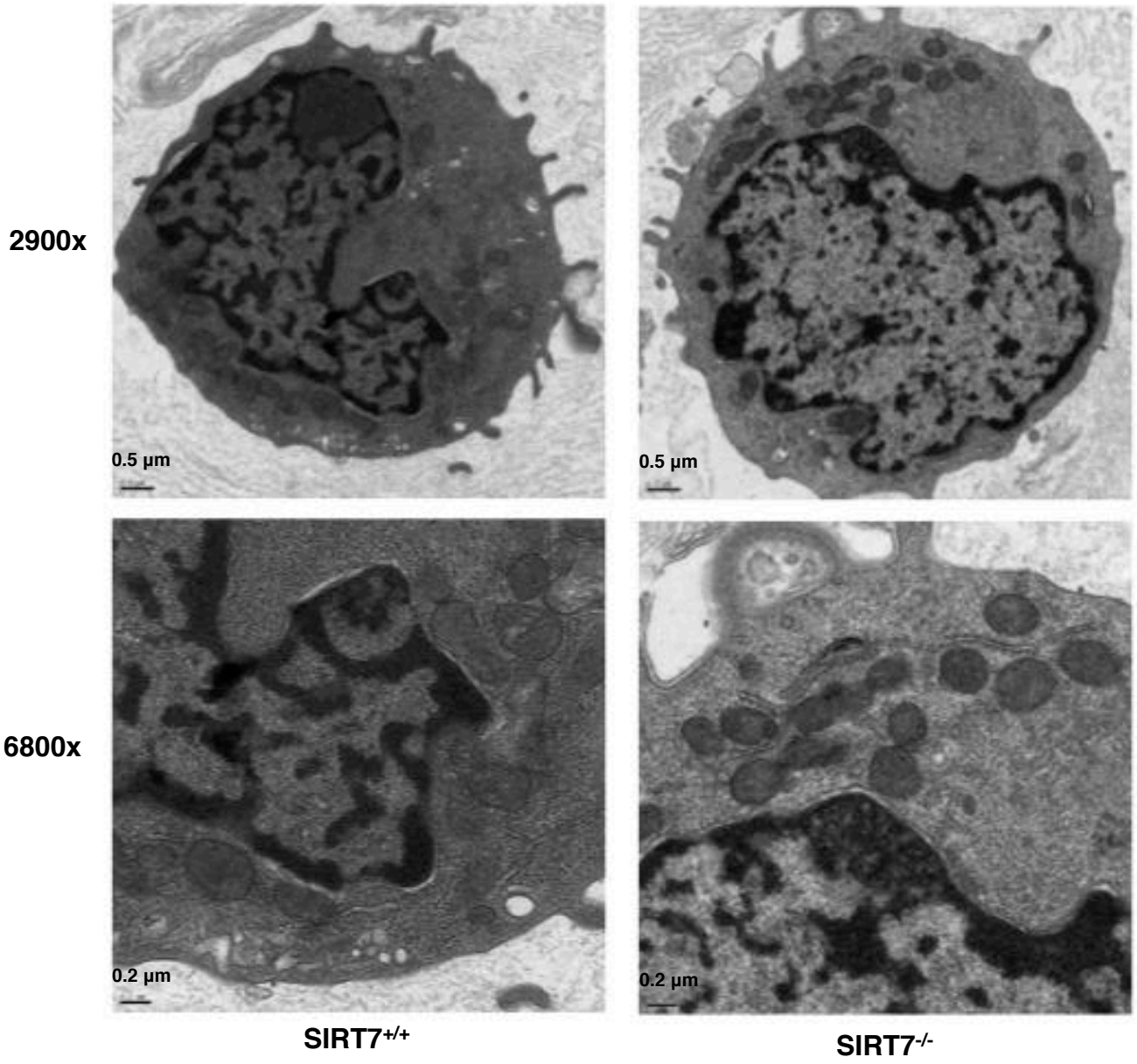

Fig. S8. SIRT7 suppresses mitochondrial number in HSCs.

Electron microscopy of SIRT7$^{-/-}$ and SIRT7$^{+/+}$ HSCs.

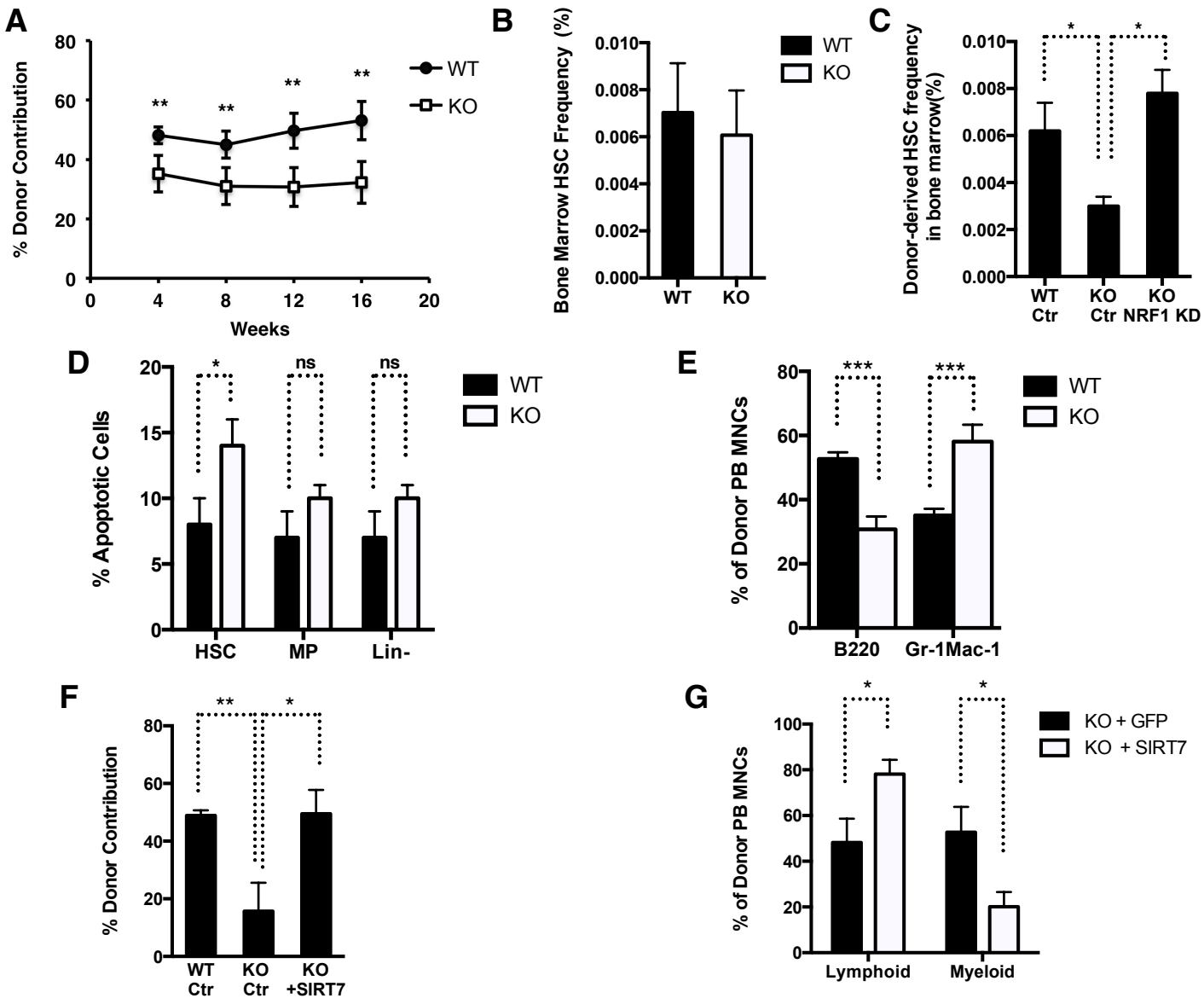

Fig. S9. SIRT7 ensures HSC maintenance.

(**A**) Competitive transplantation using HSCs isolated from SIRT7$^{+/+}$ and SIRT7$^{-/-}$ mice as donors showing reduced reconstitution capacity of SIRT7$^{-/-}$ HSCs. n=15.
(**B**) HSCs frequency in the bone marrow of SIRT7$^{+/+}$ and SIRT7$^{-/-}$ mice determined via flow cytometry. n = 4.
(**C**) SIRT7$^{+/+}$ or SIRT7$^{-/-}$ HSCs transduced with NRF1 KD lentivirus or control lentivirus were used as donors in a competitive transplantation assay. Data shown are the frequency of donor-derived HSCs in the bone marrow of recipient mice. n=6.
(**D**) Annexin V staining showing increased apoptosis in SIRT7$^{-/-}$ HSCs under transplantation stress. n=7.
(**E**) Competitive transplantation using HSCs isolated from SIRT7$^{+/+}$ and SIRT7$^{-/-}$ mice as donors.
Data shown are the distribution of donor-derived myeloid or lymphoid lineage in the peripheral blood of transplant recipients. n=15.
(**F** and **G**) SIRT7$^{+/+}$ or SIRT7$^{-/-}$ HSCs transduced with SIRT7 lentivirus or control lentivirus were used as donors in a competitive transplantation assay. Data shown are the percentage of total donor-derived contribution (F) and donor-derived mature hematopoietic subpopulations (G) in the peripheral blood of recipients. n=7.
Error bars represent SE. *: $p<0.05$. **: $p<0.01$. ***: $P<0.001$. ns: $p>0.05$.

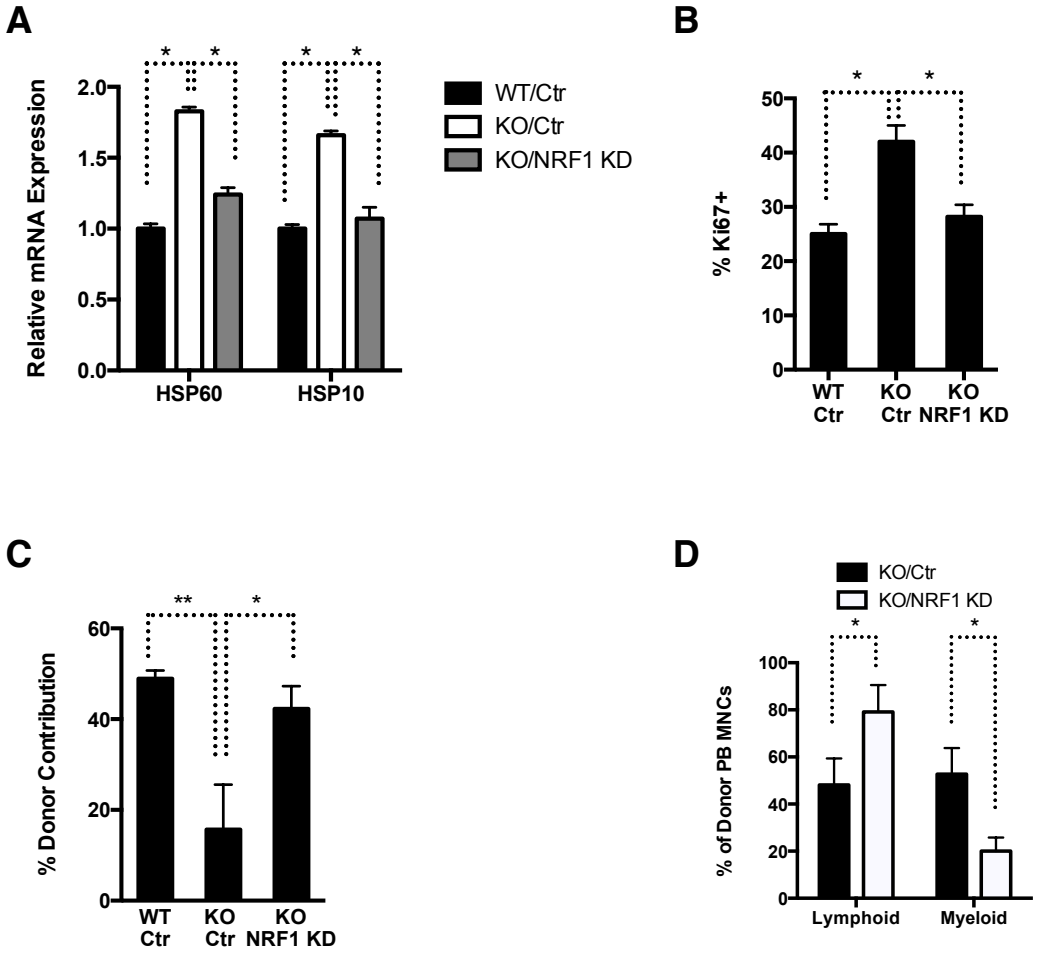

Fig. S10. SIRT7 represses NRF1 activity to ensure HSC maintenance.

(**A** to **D**) SIRT7$^{+/+}$ or SIRT7$^{-/-}$ HSCs transduced with NRF1 KD lentivirus or control lentivirus were used as donors in a competitive transplantation assay. Data shown are qPCR analyses of UPR^{mt} gene expression (A) and cell cycle analysis with Ki67 staining (B) of donor-derived HSCs, the percentage of total donor-derived contribution (C) and donor-derived mature hematopoietic subpopulations (D) in the peripheral blood of recipients. n=7.
Error bars represent SE. *: $p<0.05$. **: $p<0.01$.

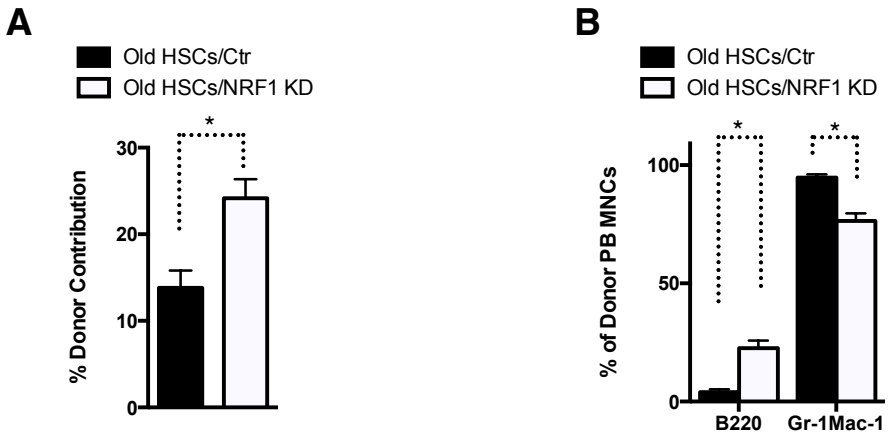

Fig. S11. HSC aging regulated by NRF1.

(**A** and **B**) Competitive transplantation using aged HSCs transduced with NRF1 KD virus or control virus as donors showing NRF1 inactivation increases reconstitution capacity and reverses myeloid-biased differentiation of aged HSCs. Data shown are the percentage of donor-derived cells in the peripheral blood of the recipients (A) and the percentage of lymphoid and myeloid cells in donor-derived cells in the peripheral blood of the recipients (B). n=7.
Error bars represent SE *: $p<0.05$.

Antibodies	Source	Catalog #
SIRT7	Abnova	H00051547
Beta Actin	Sigma	A2066
Flag	Sigma	F1804
IgG	Santa Cruz	SC-2027
RPS20	Abcam	Ab74700
NRF-1	Proteintech	12482-1-AP
MRPL24	Proteintech	16224-1-AP
GFM2	Proteintech	16941-1-AP
ClpP	Proteintech	15698-1-AP
HSP60	Cell Signaling	12165S
OTC	Santa Cruz	SC-102051

FACS Antibodies & Reagents	Source	Catalog #	Clone #
CD45.1 PerCP	Biolegend	110726	A20
Streptavidin PerCP	Biolegend	405213	
Mac1 PerCP	Biolegend	101230	M1/70
CD3 Pacific Blue	Biolegend	100214	17A2
Sca1 Pacific Blue	Biolegend	108120	D7
Streptavidin APC-Cy7	Biolegend	405208	
c-Kit APC-Cy7	Biolegend	105826	2B8
CD45.2 Cy7-PE	Biolegend	109830	104
CD150 Cy7-PE	Biolegend	115914	TC15-12F12.2
Gr1 Cy7-PE	Biolegend	108416	RB6-8C5
c-Kit Cy7-PE	Biolegend	105813	2B8
Streptavidin Cy7-PE	Biolegend	405206	
CD3 Biotin	Biolegend	100304	145-2C11
B220 Biotin	Biolegend	103204	RA3-6B2
Gr1 Biotin	Biolegend	108404	RB6-8C5
CD8a Biotin	Biolegend	100704	53-6.8
Mac1 Biotin	Biolegend	101204	M1/70
Ter119 Biotin	Biolegend	116204	TER-119
CD4 Biotin	Biolegend	100404	GK1.5
CD48 FITC	Biolegend	103404	HM48-1
Gr1 FITC	Biolegend	108406	RB6-8C5
CD45.2 FITC	eBioscience	11-0454-85	104
AnnexinV FITC	Biolegend	640906	
Ki67 A488	Biolegend	350508	Ki-67
CD150 PE	Biolegend	115904	TC15-12F12.2
CD45.1 PE	Biolegend	110708	A20
Mac1	Biolegend	101208	M1/70
c-Kit APC	Biolegend	105812	2B8
B220 APC	Biolegend	103212	RA3-6B2
Ki67 APC	Biolegend	350514	Ki-67
AnnexinV APC	Biolegend	640920	
CD48 A647	Biolegend	103416	HM48-1
Fixation buffer	Biolegend	420801	
Permeabilization wash buffer	Biolegend	421002	
AnnexinV binding buffer	Biolegend	422201	
7AAD	Biolegend	420404	
BrdU labeling reagent	Invitrogen	000103	

Table S1. Antibodies used in this study.

Gene	Primer	Sequence
SIRT7 (human)	Forward	CGCCAAATACTTGGTCGTCT
	Reverse	CCCTTTCTGAAGCAGTGTCC
ClpP (human)	Forward	CTCTTCCTGCAATCCGAGAG
	Reverse	GGATGTACTGCATCGTGTCG
Hsp10 (human)	Forward	CAGTAGTCGCTGTTGGATCG
	Reverse	TGCCTCCATATTCTGGGAGA
Hsp60 (human)	Forward	TGACCCAACAAAGGTTGTGA
	Reverse	CATACCACCTCCCATTCCAC
mtDnaJ(human)	Forward	CGAAATGGCAGAAGAAGAGG
	Reverse	TGCATGCACTACAGAGCACA
Grp78 (human)	Forward	TCATCGGACGCACTTGGAA
	Reverse	CAACCACCTTGAATGGCAAGA
ClpP (mouse)	Forward	CTGCCCAATTCCAGAATCAT
	Reverse	TGTAGGCTCTGCTTGGTGTG
Hsp10 (mouse)	Forward	CCAAAGGTGGCATTATGCTT
	Reverse	TGACAGGCTCAATCTCTCCA
Hsp60 (mouse)	Forward	ACCTGTGACAACCCCTGAAG
	Reverse	TGACACCCTTTCTTCCAACC
mtDnaJ (mouse)	Forward	GAGCTGAAGAAGGCATACCG
	Reverse	CAGCTCTCGCTTCTCTGGAT
ND4 (mtDNA) (mouse)	Forward	GGAACCAAACTGAACGCCTA
	Reverse	ATGAGGGCAATTAGCAGTGG
b2 microglobulin (nDNA) (Mouse)	Forward	TCATTAGGGAGGAGCCAATG
	Reverse	ATCCCCTTTCGTTTTTGCTT
SIRT7 (mouse)	Forward	CCATGGGAAGTGTGATGATG
	Reverse	TCCTACTGTGGCTGCCTTCT
MRPL16	Forward	ACATACGGGGACCTTCCACT
	Reverse	AAACATGTTCTTGGGGTCCA
MRPL20	Forward	GAACATGAGGACCCTCTGGA
	Reverse	CCGCTAGGACTTTCCTGTTG
MRPL24	Forward	GGGGAACCATGATCCCTAGT
	Reverse	AATTCTCCCTGATCGTGTGG
MRPS31	Forward	GAGGAAGAGTCAAGGGCACA
	Reverse	CTGAATCCGAAGCTCTGGTC
MRPS33	Forward	ATATGCCTTCCGCATGTCTC
	Reverse	GCCAAGGGCAGTTCACTAAA
CytC	Forward	AAGTGTTCCCAGTGCCACA
	Reverse	GTTCTTATTGGCGGCTGTGT
POLRMT	Forward	AAAGCCCAACACACGTAAGC
	Reverse	GTGCACAGAGACGAAGGTCA
TFAM	Forward	TGGCAAGTTGTCCAAAGAAA
	Reverse	ACGCTGGGCAATTCTTCTAA
TFB1M	Forward	CTCCCTTGATACAGCCCAAG
	Reverse	TGCGCTTCAGGGAATAACAT
TFB2M	Forward	AGATCCCGGAAATCCAGACT
	Reverse	CTACGCTTTGGGTTTTCCAG
TIMM17A	Forward	AGGGCTGTTTTCCATGATTG
	Reverse	CCACTGGTCCATTTCTTGCT
NRF1	Forward	CCCAGGCTCAGCTTCGGGCA
	Reverse	GCTCTTCTGTGCGGACATCAC
tRNALeu (mtDNA) (human)	Forward	CACCCAAGAACAGGGTTTGT
	Reverse	TGGCCATGGGTATGTTGTTA
β2-microglobulin (nDNA) (human)	Forward	TGCTGTCTCCATGTTTGATGTATCT
	Reverse	TCTCTGCTCCCCACCTCTAAGT
16S rRNA (mtDNA) (human)	Forward	GCCTTCCCCCGTAAATGATA
	Reverse	TTATGCGATTACCGGGCTCT

Table S2. Primers used for qPCR analysis in this study.

Target	Primer	Sequence
γ-tubulin	Forward	ACGGGTTTCATCATGTTTGTT
	Reverse	GGCAGATCCCCTGAGGTC
RPS20	Forward	AAGTTCTTTCTTTTTGAGGAAGACG
	Reverse	GAACAGCGGTGAGTCAGGA
GFM2	Forward	CGGGACAGGAAAGAGTCACC
	Reverse	CGGAAAACAGAGGCTCGGAA
mRPL24	Forward	TGAACAGGAAGCCACAACCA
	Reverse	GAGGCCGCTGGGAATTGTAG
NME1	Forward	CCGTAATACTTGGCTCTCGAA
	Reverse	GAATAGACCTGCATGAAGTGAGG
HSP60	Forward	CAGCGACTACTGTTGCTTGC
	Reverse	ACAGGCAGGACAAGCGTTTA
TFB1M	Forward	CCTAGTCCACCCGGCTCT
	Reverse	GAGGAACCTGCGAGACCTAA
TFB2M	Forward	ACGGTCCACTCACAATCCTC
	Reverse	CCCACGTGGAACATTTTCTG
Cytc	Forward	CCGTACACCCTAACATGCTC
	Reverse	TGGCACAACGAACACTCC
mRPL16	Forward	TCTTCTGGGGAAAGACTGGA
	Reverse	TGAGTTCCTGCGGTCAAAG
mRPL20	Forward	CGAGTTCAGGAGCACAACTG
	Reverse	GTCAGCCCCTGCGATACTT
ClpP	Forward	ATGTGGCCCGGAATATTGGT
	Reverse	CAGGCCGTTCTGGAGTGTC
HSP10	Forward	AGAGGAGGAAGGCCCACTC
	Reverse	CTGCACTCTGTCCCTCACTC

Table S3. PCR primers used for ChIP analysis in this study.

References

1. C. J. Kenyon, The genetics of ageing. *Nature* **464**, 504–512 (2010). Medline doi:10.1038/nature08980

2. C. López-Otín, M. A. Blasco, L. Partridge, M. Serrano, G. Kroemer, The hallmarks of aging. *Cell* **153**, 1194–1217 (2013). Medline doi:10.1016/j.cell.2013.05.039

3. J. Vijg, J. Campisi, Puzzles, promises and a cure for ageing. *Nature* **454**, 1065–1071 (2008). Medline doi:10.1038/nature07216

4. C. D. Folmes, P. P. Dzeja, T. J. Nelson, A. Terzic, Metabolic plasticity in stem cell homeostasis and differentiation. *Cell Stem Cell* **11**, 596–606 (2012). Medline doi:10.1016/j.stem.2012.10.002

5. L. Liu, T. H. Cheung, G. W. Charville, B. M. Hurgo, T. Leavitt, J. Shih, A. Brunet, T. A. Rando, Chromatin modifications as determinants of muscle stem cell quiescence and chronological aging. *Cell Reports* **4**, 189–204 (2013). Medline

6. A. E. Webb, E. A. Pollina, T. Vierbuchen, N. Urbán, D. Ucar, D. S. Leeman, B. Martynoga, M. Sewak, T. A. Rando, F. Guillemot, M. Wernig, A. Brunet, FOXO3 shares common targets with ASCL1 genome-wide and inhibits ASCL1-dependent neurogenesis. *Cell Reports* **4**, 477–491 (2013). Medline doi:10.1016/j.celrep.2013.06.035

7. M. F. Barber, E. Michishita-Kioi, Y. Xi, L. Tasselli, M. Kioi, Z. Moqtaderi, R. I. Tennen, S. Paredes, N. L. Young, K. Chen, K. Struhl, B. A. Garcia, O. Gozani, W. Li, K. F. Chua, SIRT7 links H3K18 deacetylation to maintenance of oncogenic transformation. *Nature* **487**, 114–118 (2012). Medline

8. R. C. Scarpulla, Transcriptional paradigms in mammalian mitochondrial biogenesis and function. *Physiol. Rev.* **88**, 611–638 (2008). Medline doi:10.1152/physrev.00025.2007

9. J. Shin, M. He, Y. Liu, S. Paredes, L. Villanova, K. Brown, X. Qiu, N. Nabavi, M. Mohrin, K. Wojnoonski, P. Li, H. L. Cheng, A. J. Murphy, D. M. Valenzuela, H. Luo, P. Kapahi, R. Krauss, R. Mostoslavsky, G. D. Yancopoulos, F. W. Alt, K. F. Chua, D. Chen, SIRT7 represses Myc activity to suppress ER stress and prevent fatty liver disease. *Cell Reports* **5**, 654–665 (2013). Medline doi:10.1016/j.celrep.2013.10.007

10. J. Y. Lu, Y. Zhang, Y. F. Shen, Inhibitory role of SirT7 in the growth of P19 cell line. *Acta Academiae Medicinae Sinicae* **31**, 724–727 (2009). Medline

11. O. Vakhrusheva, D. Braeuer, Z. Liu, T. Braun, E. Bober, Sirt7-dependent inhibition of cell growth and proliferation might be instrumental to mediate tissue integrity during aging. *J. Physiol. Pharmacol.* **59** (Suppl 9), 201–212 (2008). Medline

12. K. Brown, S. Xie, X. Qiu, M. Mohrin, J. Shin, Y. Liu, D. Zhang, D. T. Scadden, D. Chen, SIRT3 reverses aging-associated degeneration. *Cell Reports* **3**, 319–327 (2013). Medline

13. W. Giblin, M. E. Skinner, D. B. Lombard, Sirtuins: Guardians of mammalian healthspan. *Trends Genet.* **30**, 271–286 (2014). Medline doi:10.1016/j.tig.2014.04.007

14. X. Qiu, K. Brown, M. D. Hirschey, E. Verdin, D. Chen, Calorie restriction reduces oxidative stress by SIRT3-mediated SOD2 activation. *Cell Metab.* **12**, 662–667 (2010). Medline doi:10.1016/j.cmet.2010.11.015

15. K. Inoki, T. Zhu, K. L. Guan, TSC2 mediates cellular energy response to control cell growth and survival. *Cell* **115**, 577–590 (2003). Medline doi:10.1016/S0092-8674(03)00929-2

16. M. Laplante, D. M. Sabatini, mTOR signaling in growth control and disease. *Cell* **149**, 274–293 (2012). Medline doi:10.1016/j.cell.2012.03.017

17. C. M. Haynes, D. Ron, The mitochondrial UPR - protecting organelle protein homeostasis. *J. Cell Sci.* **123**, 3849–3855 (2010). Medline doi:10.1242/jcs.075119

18. Q. Zhao, J. Wang, I. V. Levichkin, S. Stasinopoulos, M. T. Ryan, N. J. Hoogenraad, A mitochondrial specific stress response in mammalian cells. *EMBO J.* **21**, 4411–4419 (2002). Medline doi:10.1093/emboj/cdf445

19. C. M. Haynes, C. J. Fiorese, Y. F. Lin, Evaluating and responding to mitochondrial dysfunction: The mitochondrial unfolded-protein response and beyond. *Trends Cell Biol.* **23**, 311–318 (2013). Medline doi:10.1016/j.tcb.2013.02.002

20. D. Ryu, Y. S. Jo, G. Lo Sasso, S. Stein, H. Zhang, A. Perino, J. U. Lee, M. Zeviani, R. Romand, M. O. Hottiger, K. Schoonjans, J. Auwerx, A SIRT7-dependent acetylation switch of GABPβ1 controls mitochondrial function. *Cell Metab.* **20**, 856–869 (2014). Medline doi:10.1016/j.cmet.2014.08.001

21. K. Miyamoto, K. Y. Araki, K. Naka, F. Arai, K. Takubo, S. Yamazaki, S. Matsuoka, T. Miyamoto, K. Ito, M. Ohmura, C. Chen, K. Hosokawa, H. Nakauchi, K. Nakayama, K. I. Nakayama, M. Harada, N. Motoyama, T. Suda, A. Hirao, Foxo3a is essential for maintenance of the hematopoietic stem cell pool. *Cell Stem Cell* **1**, 101–112 (2007). Medline doi:10.1016/j.stem.2007.02.001

22. S. M. Chambers, C. A. Shaw, C. Gatza, C. J. Fisk, L. A. Donehower, M. A. Goodell, Aging hematopoietic stem cells decline in function and exhibit epigenetic dysregulation. *PLOS Biol.* **5**, e201 (2007). Medline doi:10.1371/journal.pbio.0050201

23. V. Janzen, R. Forkert, H. E. Fleming, Y. Saito, M. T. Waring, D. M. Dombkowski, T. Cheng, R. A. DePinho, N. E. Sharpless, D. T. Scadden, Stem-cell ageing modified by the cyclin-dependent kinase inhibitor p16INK4a. *Nature* **443**, 421–426 (2006). Medline

24. J. Oh, Y. D. Lee, A. J. Wagers, Stem cell aging: Mechanisms, regulators and therapeutic opportunities. *Nat. Med.* **20**, 870–880 (2014). Medline doi:10.1038/nm.3651

25. R. A. Signer, S. J. Morrison, Mechanisms that regulate stem cell aging and life span. *Cell Stem Cell* **12**, 152–165 (2013). Medline doi:10.1016/j.stem.2013.01.001

26. J. A. Dahl, P. Collas, A quick and quantitative chromatin immunoprecipitation assay for small cell samples. *Front. Biosci.* **12**, 4925–4931 (2007). Medline doi:10.2741/2438

27. C. Zhao, A. Chen, C. H. Jamieson, M. Fereshteh, A. Abrahamsson, J. Blum, H. Y. Kwon, J. Kim, J. P. Chute, D. Rizzieri, M. Munchhof, T. VanArsdale, P. A. Beachy, T. Reya, Hedgehog signalling is essential for maintenance of cancer stem cells in myeloid leukaemia. *Nature* **458**, 776–779 (2009). Medline doi:10.1038/nature07737

28. L. Lai, T. C. Leone, C. Zechner, P. J. Schaeffer, S. M. Kelly, D. P. Flanagan, D. M. Medeiros, A. Kovacs, D. P. Kelly, Transcriptional coactivators PGC-1α and PGC-lβ control overlapping programs required for perinatal maturation of the heart. *Genes Dev.* **22**, 1948–1961 (2008). Medline doi:10.1101/gad.1661708

29. V. Venegas, J. Wang, D. Dimmock, L. J. Wong, Real-time quantitative PCR analysis of mitochondrial DNA content. *Curr. Protoc. Hum. Genet.* Chapter 19, Unit 19.7 (2011). doi:10.1002/0471142905.hg1907s68